



*Supplement of*

## **Comprehensive mapping and characteristic regimes of aerosol effects on the formation and evolution of pyro-convective clouds**

**D. Chang et al.**

*Correspondence to:* H. Su ([h.su@mpic.de](mailto:h.su@mpic.de))

The copyright of individual parts of the supplement might differ from the CC-BY 3.0 licence.

## Supplementary Material

### 1. Comparison with 3-D simulations

In this study, we have demonstrated the importance of ensemble simulations in determining the regime dependence and nonlinearities of aerosol effects. The ensemble simulation method will advance the understanding of aerosol-cloud interactions compared with the case study method commonly used nowadays. However, results from ensemble simulations should be used with caveats. One reason is that aerosol effects may differ under distinct meteorological conditions or other influencing factors. The other reason is that the reliability of ensemble studies depends on the performance of cloud models, of which results may differ for different model setup (e.g., microphysics, dynamics, model dimensions, etc.). Here, we show that the influence of model dimensions on the calculated regime dependence of aerosol effects. The results from three-dimensional simulations will be presented and compared with the two-dimensional results in the main text. As the three-dimensional simulations are extremely computational expensive, only 99 cases ( $11 N_{\text{CN}} \times 9 FF$  values) were performed to evaluate the response of the clouds and precipitation to the aerosol concentration and updrafts.

As shown in Fig. S1a, there are also three-different regimes involved for the number concentration of cloud droplets ( $N_{\text{CD}}$ ), similar to the 2-D case (Fig. 7a). In the upper-left sector,  $N_{\text{CD}}$  is very sensitive to  $N_{\text{CN}}$ , which is the aerosol-limited regime. In the lower-right sector,  $N_{\text{CD}}$  is mainly controlled by fire forcing, which is the updraft-limited regime. In the region along the diagonal,  $N_{\text{CD}}$  is sensitive to both  $N_{\text{CN}}$  and fire forcing, which is the transitional regime. However, the mass concentration of cloud droplets ( $M_{\text{CD}}$ ) is less sensitive to  $N_{\text{CN}}$  (Fig. S1b), compared with  $N_{\text{CD}}$ . Only when  $N_{\text{CN}}$  is smaller than  $1,000 \text{ cm}^{-3}$ , an increase in  $N_{\text{CN}}$  leads to the enhanced  $M_{\text{CD}}$ . When  $N_{\text{CN}}$  is larger, fire forcing is the predominant factor that controls the change of  $M_{\text{CD}}$ .

Based on the calculated  $RS(N_{\text{CN}})$  to  $RS(FF)$  ratio, the formation of raindrops is mainly controlled by the fire forcing. The number concentration of raindrops ( $N_{\text{RD}}$ ) is mostly proportional to fire forcing, and the aerosol effect is nearly negligible (Fig. S2a). For mass concentration ( $M_{\text{RD}}$ ), an increase in aerosols could slightly boost the production of raindrops when  $N_{\text{CN}}$  is very low (Fig. S2b). This is consistent with 2-D simulations.

29           The contours of the total frozen particles (including ice, snow, graupel and hail) as a function  
30 of  $N_{CN}$  and fire forcing indicate that the production of frozen particles is in general controlled by fire  
31 forcing (Fig. S3). Similar to Fig. 12, an increase in  $N_{CN}$  leads to an enhancement in  $N_{FP}$  and  $M_{FP}$ ,  
32 particularly when  $N_{CN}$  is in a low level.

33           Different from the response of rain rate to aerosols derived from 2-D simulations, the aerosol  
34 concentrations tend to play a negative role in the rain rate (Fig. S4). When  $N_{CN}$  is larger than 5,000  
35  $\text{cm}^{-3}$ , its effect is negligible.

47 Figure captions:

48 Figure S1. Number (a) and mass concentration (b) of cloud droplets calculated as a  
49 function of aerosol number concentration ( $N_{CN}$ ) and updraft velocity (represented by  $FF$ )  
50 from three-dimensional simulations.

51 Figure S21. Same as Fig. S1, but for raindrops.

52 Figure S3. Same as Fig. S1, but for total frozen particles.

53 Figure S4. Same as Fig. S1, but for rain rate.

54

55

56

57

58

59

60

61

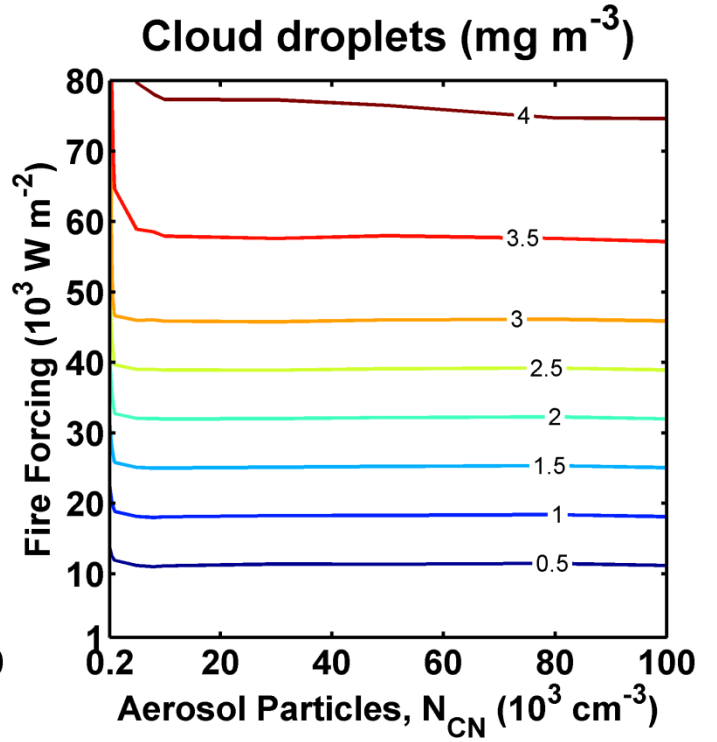
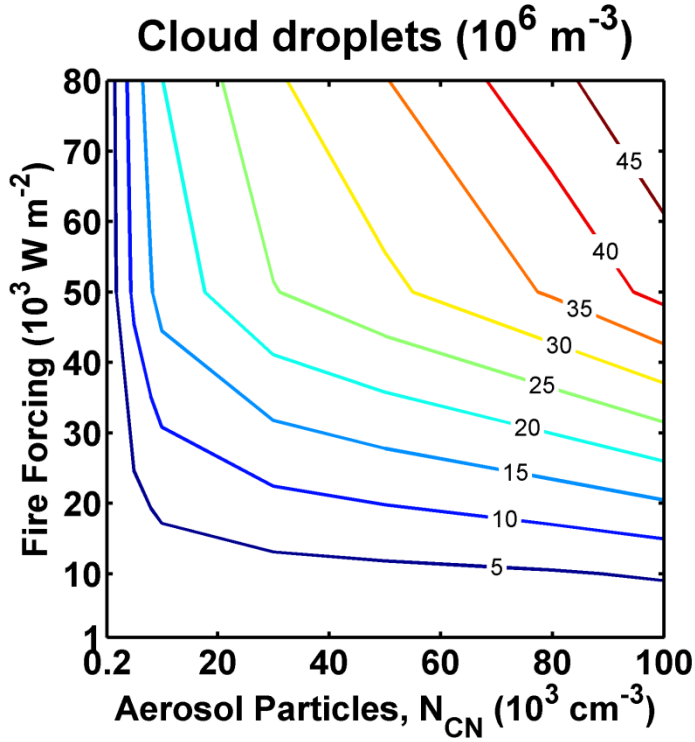
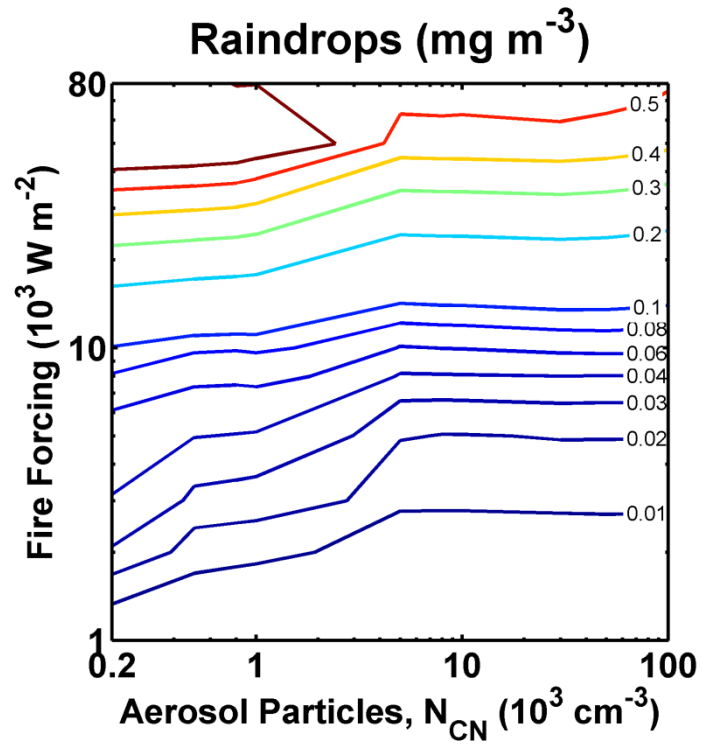
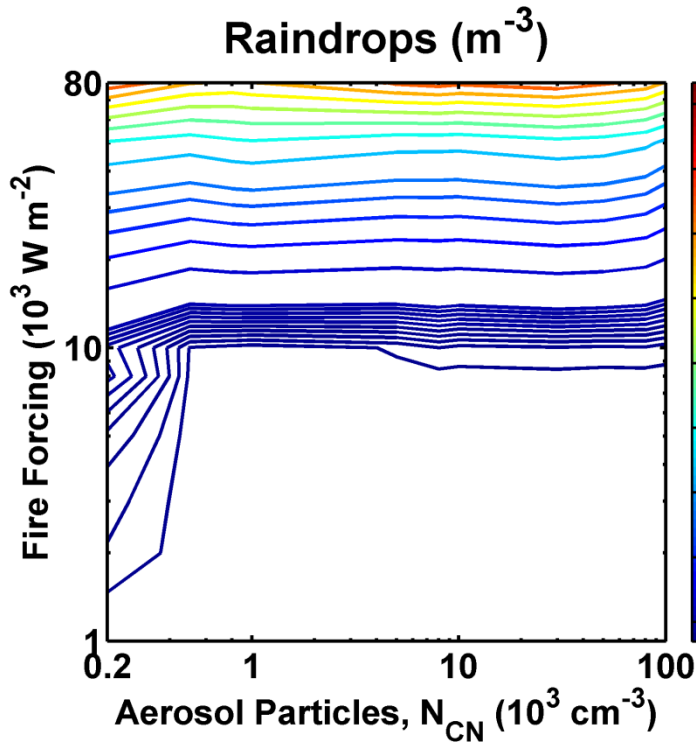


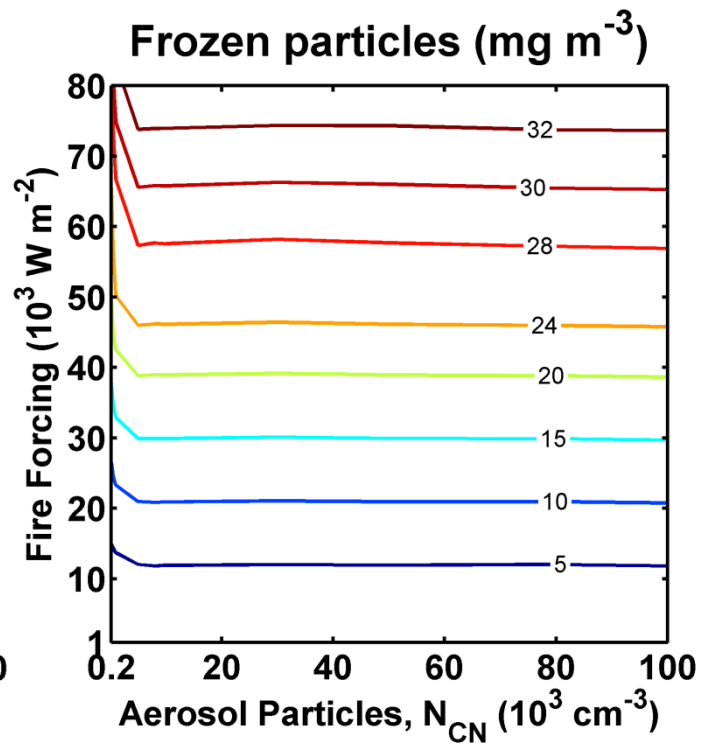
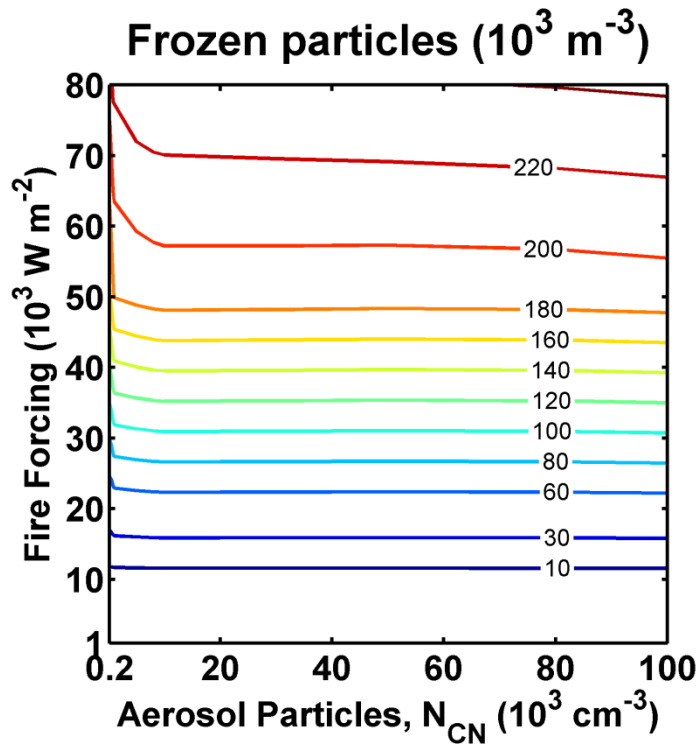
Figure S1. Number (a) and mass concentration (b) of cloud droplets calculated as a function of aerosol number concentration ( $N_{\text{CN}}$ ) and updraft velocity (represented by  $FF$ ) from three-dimensional simulations.



(a)

(b)

Figure S22. Same as Fig. S1, but for raindrops.



90 (a)

90 (b)

91 Figure S3. Same as Fig. S1, but for total frozen particles.

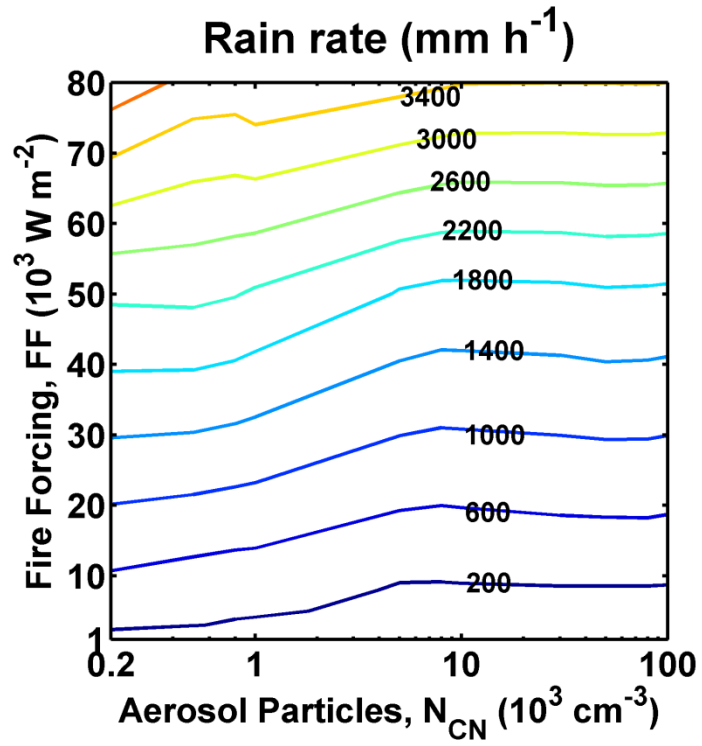


Figure S4. Same as Fig. S1, but for rain rate.

93

94